

## Sliding charge-density waves as rough growth fronts

K. L. Ringland, A. C. Finnefrock, Y. Li, and J. D. Brock

*School of Applied & Engineering Physics, Cornell University, Ithaca, New York 14853*

S. G. Lemay and R. E. Thorne

*Department of Physics, Cornell University, Ithaca, New York 14853*

(Received 12 October 1999)

Using high-resolution x-ray scattering techniques, we have measured the transverse static structure factor of the sliding charge-density wave (CDW) in  $\text{NbSe}_3$ . For temperatures between 70 and 120 K and for applied currents up to 40 times the threshold current for sliding, the scattering peak for the sliding CDW is significantly broader than that for the pinned CDW, indicating that the sliding state is less correlated than the pinned state. Using scaling analysis, we show that the CDW phase roughness exponent  $\alpha$  rises from  $0.60 \pm 0.01$  in the pinned state to  $0.80 \pm 0.01$  in the sliding state, indicating that the phase fronts of the sliding CDW are significantly rougher than those of the pinned CDW.

There are several systems of current interest (including charge- and spin-density waves, type-II superconductor vortex lattices, and Wigner crystals<sup>1-4</sup>) which have ordered electrical or magnetic states at low temperatures. Ideally, these systems exhibit long-range order and can slide freely with respect to the underlying crystal. However, the presence of impurities and defects creates a rugged potential-energy terrain, and the competition between the ensuing quenched random-field and elastic restoring forces results in many rich and complex physical phenomena. Most notably, the ordered system distorts in order to accommodate the random field, though this accommodation is limited by the energy cost of the distortion. The result is that long-range order is destroyed and the system is pinned such that a finite drive field is required to induce sliding. Furthermore, when driven into the sliding state, the response of the system will depend nontrivially on the rate of movement, the rate of propagation of fluctuations, and the strength of the random field. The expectation has been that if the system is driven to slide at high velocities, the effects of the stationary random field will be washed out, and the system will become well-ordered or *smooth*. Direct structural evidence of this exists for superconductor vortex lattices,<sup>5</sup> but has been lacking for the other systems of interest. Since the physical principles governing all of the above systems are very similar, it is expected that the behavior seen for the vortex lattices should be observed in the other systems as well. To test this, we have chosen to study the charge-density wave (CDW) because CDW structural information is directly accessible via high-resolution x-ray scattering. The structure of the zero-field-cooled pinned state has been studied,<sup>6</sup> as has the relaxational dynamics of the pinning transition;<sup>7</sup> this paper focuses on the structure of the sliding CDW. We show here that at high velocities the sliding CDW in  $\text{NbSe}_3$  does not exhibit a transition into an ordered state as expected, but instead becomes highly disordered with *rough* phase fronts.

The CDW state is a periodic modulation of the conduction electron density with an accompanying modulation of the underlying crystal lattice. One indication of the presence of a CDW is non-Ohmic conduction in response to an ap-

plied electric field which is greater than a threshold field.<sup>8-10</sup> For small currents, the CDW remains pinned to the impurities and defects in the underlying crystal. For large currents, however, the CDW detaches from the pinning field and slides (conducts), lowering the crystal's differential resistance. Since CDW current corresponds to CDW velocity, large applied currents imply large CDW velocities. Another signature of a CDW is the presence of a lattice-distortion wave in the crystal lattice. Through studying the resulting x-ray scattering peaks, we can gain information about the structure of the CDW in both the pinned and driven states.

In the simplest form of the CDW distortion, the atomic positions are offset by  $\mathbf{u} = \mathbf{u}_0 \sin[\mathbf{Q} \cdot \mathbf{r} + \phi(\mathbf{r}, t)]$ . Here  $\mathbf{Q} = 2k_F \hat{n}$  is the CDW wave vector,  $k_F$  is the Fermi wave number, and  $\phi$  is the phase of the CDW. The inclusion of this additional Fourier component into the crystal lattice creates scattering peaks that flank the undistorted crystal's Bragg peaks. The static structure function of the CDW scattering peak can then be easily derived, yielding

$$S(\mathbf{q}) \sim |J_1(\mathbf{q} \cdot \mathbf{u}_0)|^2 \int d^3r e^{i(\mathbf{q} - \mathbf{G} \pm \mathbf{Q}) \cdot \mathbf{r}} e^{-g(\mathbf{r})}, \quad (1)$$

where  $g(\mathbf{r}) \equiv \frac{1}{2} \langle [\phi(\mathbf{r}) - \phi(\mathbf{0})]^2 \rangle$  is the phase difference function,  $J_1(x)$  is the Bessel function of order 1,  $\mathbf{q}$  is the x-ray scattering vector, and  $\mathbf{G}$  is a reciprocal-lattice vector of the undistorted crystal. Equation (1) assumes a Gaussian probability distribution for the phase fluctuations, but this treatment also holds well for small fluctuations with a zero mean. We also assume that the amplitude  $\mathbf{u}_0$  is constant since the temperature range studied is significantly below that at which the CDW forms. Given these assumptions, the line shape of the CDW peak is determined exclusively by  $g(\mathbf{r})$ .

The anisotropic metal  $\text{NbSe}_3$  exhibits a phase transition to an incommensurate CDW state at  $T = 145$  K, and has satellite peaks with  $\mathbf{Q} = (0 \ 0.243 \ 0)$ .<sup>11</sup> We elected to study  $\text{NbSe}_3$  because its CDW exhibits sliding conduction and because it is available in nearly perfect, single-crystal whiskers. The macroscopic sample dimensions were approximately  $2 \mu\text{m} \times 20 \mu\text{m} \times 5 \text{mm}$ . Residual resistance ratios were ap-

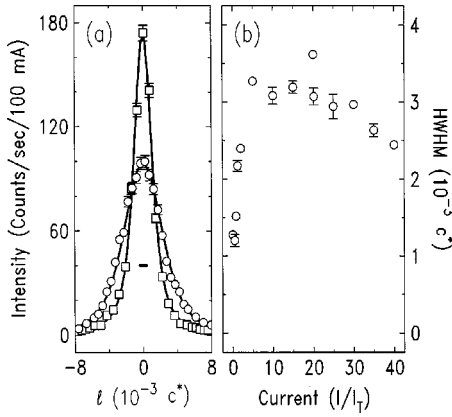


FIG. 1. (a) Transverse scans of the sliding CDW (circles,  $30I_T$ ) and pinned CDW (squares, zero current). Lines are the best fit to Eq. (2). The horizontal bar indicates the resolution (pure  $\text{NbSe}_3$ , 100 K). (b) Width of the CDW scattering peak, resolution removed, for the same sample and temperature.

proximately 300 for the pure samples and 70 for samples doped with tantalum at a density of  $3 \times 10^{18} \text{ cm}^{-3}$ .<sup>12</sup> Typical threshold field values at 120 K were  $0.08 \text{ V cm}^{-1}$  for the pure samples and  $0.3 \text{ V cm}^{-1}$  for the doped samples.

The white x-ray beam generated by the National Synchrotron Light Source (NSLS) storage ring was doubly focused at the sample position by a toroidal mirror, and 8.25-keV x rays were selected by a double-crystal Ge(111) monochromator. A set of slits limited the height of the illuminated region to 0.4 mm (the width of the whisker sets the other dimension). The bulk crystal mosaic dominated the transverse resolution, and the longitudinal and out-of-plane resolutions were determined by a final set of slits. The resulting resolution function is highly asymmetric and effectively integrates over the longitudinal and out-of-plane directions in Eq. (1), collapsing the three-dimensional integral to one dimension.<sup>13</sup> Typically the CDW scattering peak was  $O(10^3)$  times more intense than the background. Currents were applied to the  $\text{NbSe}_3$  sample via contacts far ( $>1$  mm) from the section illuminated by the x-ray beam.

Each data set consists of transverse scans of the CDW scattering peak in the  $\mathbf{a}^*$  or  $\mathbf{c}^*$  direction. Scans were taken at temperatures ranging from 70 to 120 K and for drive currents from 0 to 40 times the threshold current for sliding,  $I_T$ .<sup>14</sup> The data presented here were taken from eight nominally pure samples and two Ta-doped samples. Figure 1(a) shows typical scans in the pinned and sliding states. The widths of the scattering peaks are insensitive to temperature and to position on the sample; however, their dependence on the strength of the drive current is significant, as shown in Fig. 1(b). The widths increase with current until at approximately  $(3-5)I_T$  they saturate. In a few samples the peak width decreases marginally ( $<20\%$ ) for  $(30-40)I_T$ ; however, it *never* becomes smaller than the pinned-state width. (At these currents, sample heating of a few degrees may affect the peak width.) Since the half width at half maximum (HWHM) is inversely proportional to the phase-phase correlation length, the sliding CDW is *less* correlated than the pinned CDW, even at high velocities.

This initial result is quite surprising. Models based on the Fukayama-Lee-Rice (FLR) Hamiltonian<sup>15</sup> have predicted

that for a weak CDW impurity interaction the random character of the pinning field dominates, yielding an exponential decay of the phase correlation in both the pinned and high-velocity limits.<sup>16-18</sup> At driving fields near threshold, it is expected<sup>19,20</sup> and observed<sup>21</sup> that the sliding state should be disordered, possibly due to plastic flow. However, at high fields the impurity interaction is renormalized, decreasing the pinning strength and increasing the degree of order relative to that in the pinned state. Increased order implies longer correlation lengths, which in turn imply narrower scattering peaks. The dynamics of the CDW can also include symmetry allowed terms that do not originate from the equilibrium FLR Hamiltonian. However, studies of such additions still yield ordered sliding states with long correlation lengths.<sup>18-20</sup>

In direct contrast, we observe that the width of the sliding CDW *always* exceeds that of the pinned CDW, refuting the notion that the sliding state is more ordered than the pinned state. Thus present microscopic models fail to capture the dominant physics of the sliding CDW. However, our previous work<sup>7</sup> has shown that the dynamic evolution of the CDW as it relaxes into the pinned state is remarkably similar to that predicted for the interface height in well-known surface growth models.<sup>22</sup> In that treatment, the CDW phase  $\phi$  corresponds to the interface height, and the phase difference function  $g(\mathbf{r})$  is analogous to the height difference function. Extending this intriguing analogy to the sliding state, consider the CDW in terms of an interaction between surfaces of constant phase and impurities that pass by rapidly (in the frame of reference of the sliding CDW), creating noise that is locally temporally and spatially random—akin to the randomness of material deposition. These phase fronts could then be self-affine, as are those in the surface growth models. The signature of such behavior would be that the phase difference function would scale with distance as  $g(\mathbf{r}) \sim r^{2\alpha}$ , where  $\alpha$  is the phase roughness exponent. A large value of  $\alpha$  implies rough phase fronts. To explore the validity of the analogy, we now apply this simple model to the sliding-state data.

Using the form  $g(\mathbf{r}) = (r/\xi)^{2\alpha}$  in Eq. (1), and integrating out the unresolved directions,<sup>13</sup> the predicted scattering intensity becomes

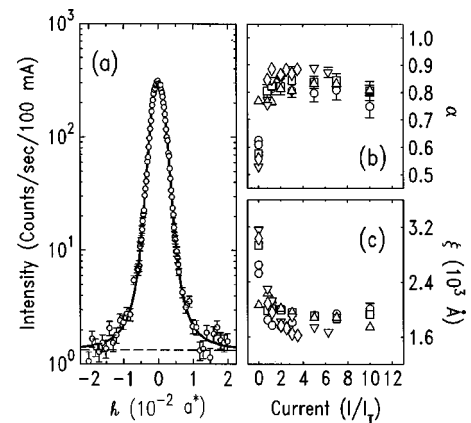


FIG. 2. (a) Transverse scan of sliding CDW with fit to Eq. (2) ( $\chi^2=1.5$ ). The dashed line shows the background (Ta-doped  $\text{NbSe}_3$ , 70 K,  $3I_T$ ). (b) Fit parameters  $\alpha$  and  $\xi$  for the same sample.  $\circ=110$  K,  $\square=100$  K,  $\triangle=90$  K,  $\nabla=80$  K, and  $\diamond=70$  K.

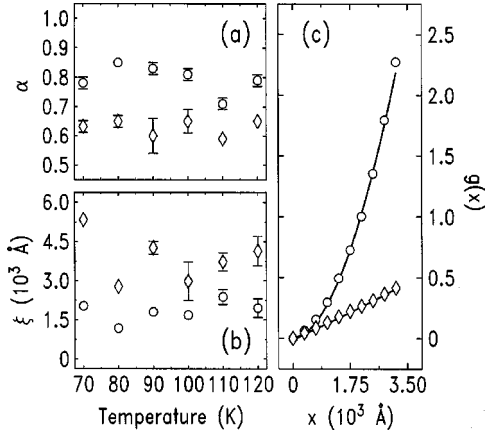


FIG. 3. (a) and (b) Average fit parameters  $\alpha$  and  $\xi$  as functions of temperature for all pure NbSe<sub>3</sub> samples with scans in the  $\mathbf{a}^*$  direction. (Note that the 80-K point is the average of many data points and is therefore weighted heavily in the averages presented in Table I.) (c) The phase difference function  $g(x)$ . Symbols are transformed data. Solid lines are fits to Eq. (2) (pure NbSe<sub>3</sub>, 90 K). For (a), (b), and (c),  $\diamond$  is the pinned state, and  $\circ$  is the sliding state.

$$I(q_{\perp}) \sim R(q_{\perp} - Q_{\perp}) \int dx e^{-i(q_{\perp} - Q_{\perp})x} e^{-(x/\xi)^{2\alpha}}, \quad (2)$$

where  $R(q_{\perp} - Q_{\perp})$  is the resolution function in the remaining transverse direction, and is convolved with the one dimensional static structure factor;  $\xi$  is the scaling constant for  $x$  (corresponding to the correlation length<sup>23</sup>); and  $Q_{\perp}$  is the peak position. The resolution function is taken to be Gaussian with a typical HWHM of  $2 \times 10^{-4} \text{ \AA}^{-1}$ .

This model describes the data extremely well, [see Fig. 2(a), solid line]. The scaling form shows marked agreement with the data throughout the entire scattering peak. This excellence of fit demonstrates that the hypothesis of self-affine phase fronts is consistent with the data.

An example of the behavior of  $\alpha$  and  $\xi$  as a function of current is shown in Figs. 2(b) and 2(c). When the current is zero, the CDW is pinned and  $\alpha \approx \frac{1}{2}$ —the value predicted<sup>16,17</sup> and observed<sup>6</sup> for the zero-field-cooled pinned state. Furthermore, the correlation length is long and in agreement with previously measured values.<sup>6</sup> When the current is nonzero, the value of the phase roughness increases, until at about  $3I_T$  it saturates at  $\alpha \approx 0.8$ , and  $\xi$  saturates at a value which is significantly smaller than that for the pinned state. This behavior is robust; it persists out to as high as  $40I_T$  and is insensitive to sample size and quality (as determined by the mode-locking spectrum).

The fit results for  $\alpha$  and  $\xi$ , averaged over several nominally pure NbSe<sub>3</sub> samples, are shown as a function of temperature in Figs. 3(a) and 3(b). Neither  $\alpha$  nor  $\xi$  are sensitive to temperature, so temperature-averaged values are given in Table I. Furthermore, the value of  $\alpha$  is insensitive to light Ta-doping, so an average for all the data yields  $\alpha = 0.60 \pm 0.01$  for the pinned state and  $\alpha = 0.80 \pm 0.01$  for the sliding state.

To interpret these results, consider Fig. 3(c) which shows  $g(x)$  for the pinned and sliding states. The symbols are the fast Fourier transform (FFT) of the scattering data (with resolution removed) plotted on a log scale, and the lines are

TABLE I. Summary of  $\alpha$  and  $\xi$  from pure and doped samples in the pinned state and the saturated region of the sliding state.

		Pure samples		Doped samples
		$\mathbf{a}^*$	$\mathbf{c}^*$	$\mathbf{a}^*$
$\alpha$	pinned	$0.62 \pm 0.01$	$0.53 \pm 0.07$	$0.59 \pm 0.02$
	sliding	$0.83 \pm 0.01$	$0.80 \pm 0.06$	$0.77 \pm 0.02$
$\xi$ ( $\text{\AA}$ )	pinned	$2920 \pm 130$	$2680 \pm 100$	$2360 \pm 100$
	sliding	$1300 \pm 70$	$840 \pm 60$	$1320 \pm 20$

$g(x)$  from the fits to Eq. (2). As the value of the phase difference function  $g(x)$  becomes larger, the degree of phase correlation in the CDW becomes smaller. One can see that the short-length-scale behavior of the CDW is similar in both the sliding and pinned states. However, for  $x \geq 700 \text{ \AA}$ , the values of  $g(x)$  for the pinned and sliding states diverge. The rapid rise of  $g(x)$  in the sliding state indicates a sudden decline in phase correlation. This requires the presence of high-frequency phase fluctuations, without which such a decline would be impossible. Therefore, a reasonable interpretation of the data is that in the sliding state high-frequency fluctuations create sharp domain walls between regions of fairly high correlation. This is the physical picture of what roughness entails in this system. In contrast, since there are fewer high-frequency fluctuations in the relatively smooth pinned state, the domain walls are broader and the decay of the phase correlation is more gradual.

The fits also yield the peak position and the integrated intensity. When the CDW depins and slides, the CDW wave vector often exhibits a slight rotation which is generally small ( $< 0.1^\circ$ ) and insensitive to temperature and position on the sample. However, the peak rotation varies greatly from sample to sample, suggesting that it is not an intrinsic effect. The integrated intensity was roughly constant with drive current; however, slow beam drift during the acquisition of the data makes accurate measurements difficult. The constancy of the integrated intensity is better supported by time-resolved data on the pinning transition.<sup>7</sup>

In summary, we have shown that the high-velocity sliding state of the CDW in NbSe<sub>3</sub> exhibits a low degree of correlation, contradicting the predictions of current theories. We have also shown that the sliding-state behavior of CDW's is well described by an empirical model very similar to those used in surface growth. Within this model, the behavior of both the pinned and sliding-state CDW's are accurately described by a scaling form for which the values of the phase-roughness exponent  $\alpha$  are  $0.60 \pm 0.01$  for the pinned state and  $0.80 \pm 0.01$  for the sliding state. The enhanced value of  $\alpha$  in the sliding state suggests that the sliding structure is rougher than the pinned structure, and that it has sharper domain walls than those in the pinned state. This surprising departure from the expected behavior raises important questions about the entire class of systems with similar physics. New microscopic models will need to address why CDW's do not reorder at high velocities, and why this differs from superconducting vortex lattices which appear to exhibit reordering.

This research was supported by NSF Grant Nos. DMR-95-01119, DMR-98-01792, and DMR-92-57466. The authors would like to thank M. Grant for valuable discussions,

and J. Jordan-Sweet and S. Lamarin for technical assistance. K.L.R. acknowledges a NSF fellowship. S.G.L. acknowledges support from NSERC. A.C.F. acknowledges support from the Cornell Center for Materials Research (NSF Grant

No. DMR-96-32275). X-ray data were collected on beam line X20A at the NSLS. The NSLS is supported by the U.S. Department of Energy, Division of Materials Sciences and Division of Chemical Sciences.

- 
- <sup>1</sup>G. Grüner, *Density Waves in Solids* (Addison-Wesley, Reading, MA, 1994), and references therein.
- <sup>2</sup>G. Grüner, *Rev. Mod. Phys.* **66**, 1 (1994).
- <sup>3</sup>G. Blatter, M. V. Feigel'man, V. B. Geshkenbein, A. I. Larkin, and V. M. Vinokur, *Rev. Mod. Phys.* **66**, 1125 (1994).
- <sup>4</sup>R.L. Willet, in *Phase Transitions and Relaxation in Systems with Competing Energy Scales*, Vol. 415 of *NATO Advanced Study Institute, Series C: Electron Solidification in Two Dimensions*, edited by T. Riste and D. Sherrington (Kluwer, Dordrecht, 1993), p. 367.
- <sup>5</sup>P. Thorel, R. Kahn, Y. Simon, and D. Cribier, *J. Phys.* **34**, 447 (1973).
- <sup>6</sup>J.D. Brock, A.C. Finnefrock, K.L. Ringland, and E. Sweetland, *Phys. Rev. Lett.* **73**, 3588 (1994). Note that the short-length-scale cutoff discussed in this reference is an extremely small effect and is unobservable in the data presented here.
- <sup>7</sup>K.L. Ringland, A.C. Finnefrock, Y. Li, J.D. Brock, S.G. Lemay, and R.E. Thorne, *Phys. Rev. Lett.* **82**, 1923 (1999).
- <sup>8</sup>H. Fröhlich, *Proc. R. Soc. London, Ser. A* **223**, 296 (1954).
- <sup>9</sup>R.M. Fleming and C.C. Grimes, *Phys. Rev. Lett.* **42**, 1423 (1979).
- <sup>10</sup>N.P. Ong and P. Monceau, *Phys. Rev. B* **16**, 3443 (1977).
- <sup>11</sup>For lattice parameters, see J.L. Hodeau, M. Marezio, C. Roucau, R. Ayroles, A. Meerschaut, J. Rouxel, and P. Monceau, *J. Phys. C* **11**, 4117 (1978).
- <sup>12</sup>J. McCarten, M. Maher, T.L. Adelman, and R.E. Thorne, *Phys. Rev. Lett.* **63**, 2841 (1989).
- <sup>13</sup>D. DiCarlo, R. E. Thorne, E. Sweetland, M. Sutton, and J. D. Brock, *Phys. Rev. B* **50**, 8288 (1994).
- <sup>14</sup>To a reasonable approximation ( $\sim 10\%$ ),  $I \propto E$ , since the resistance of NbSe<sub>3</sub> is dominated by the Ohmic contribution.
- <sup>15</sup>H. Fukuyama and P.A. Lee, *Phys. Rev. B* **17**, 535 (1978); P.A. Lee and T.M. Rice, *ibid.* **19**, 3970 (1979).
- <sup>16</sup>L.J. Sham and B.R. Patton, *Phys. Rev. B* **13**, 3151 (1976).
- <sup>17</sup>K.B. Efetov and A.I. Larkin, *Zh. Éksp. Teor. Fiz.* **72**, 2350 (1977) [*Sov. Phys. JETP* **45**, 1236 (1977)].
- <sup>18</sup>Lee-Wen Chen, L. Balents, M.P.A. Fisher, and M.C. Marchetti, *Phys. Rev. B* **54**, 12 798 (1996).
- <sup>19</sup>L. Balents and M.P.A. Fisher, *Phys. Rev. Lett.* **75**, 4270 (1995).
- <sup>20</sup>Igor S. Aranson, Stefan Scheidl, and Valerii M. Vinokur, *Phys. Rev. B* **58**, 14 541 (1998).
- <sup>21</sup>R.M. Fleming, R.G. Dunn, and L.F. Schneemeyer, *Phys. Rev. B* **31**, R4099 (1985).
- <sup>22</sup>*Dynamics of Fractal Surfaces*, edited by F. Family and T. Vicsek (World Scientific, Singapore, 1990).
- <sup>23</sup>The relationship between the correlation length ( $L$ ) and  $\xi$  varies with the scaling exponent. If  $L$  is  $1/\text{HWHM}$  of the scattering peak, then, for  $\alpha = \frac{1}{2}$ , corresponding to a Lorentzian peak shape,  $L = \xi$  and for  $\alpha = 1$ , corresponding to a Gaussian peak shape  $L = \xi/2 \ln 2$ .